

# **SIP: Site in Pieces – A Dataset of Disaggregated Construction-Phase 3D Scans for Semantic Segmentation and Scene Understanding**

Seongyong Kim, S.M. ASCE<sup>1</sup>, and Yong Kwon Cho, F. ASCE<sup>2\*</sup>

<sup>1</sup>Graduate Student, School of Civil and Environmental Engineering, Georgia Institute of Technology, GA, E-mail: skim3310@gatech.edu

<sup>2</sup>Professor, School of Civil and Environmental Engineering, Georgia Institute of Technology, GA, E-mail: yong.cho@ce.gatech.edu (Corresponding Author)

## **ABSTRACT**

Accurate 3D scene interpretation in active construction sites is essential for progress monitoring, safety assessment, and digital twin development. LiDAR is widely used in construction because it offers advantages over camera-based systems, performing reliably in cluttered and dynamically changing conditions. Yet most public datasets for 3D perception are derived from densely fused scans with uniform sampling and complete visibility, conditions that do not reflect real construction sites. Field data are often collected as isolated single-station LiDAR views, constrained by safety requirements, limited access, and ongoing operations. These factors lead to radial density decay, fragmented geometry, and view-dependent visibility—characteristics that remain underrepresented in existing datasets. This paper presents SIP, Site in Pieces, a dataset created to reflect the practical constraints of LiDAR acquisition during construction. SIP provides indoor and outdoor scenes captured with a terrestrial LiDAR scanner and annotated at the point level using a taxonomy tailored to construction environments: A. Built Environment, B. Construction Operations, and C. Site Surroundings. The dataset includes both structural components and slender temporary objects such as scaffolding, MEP piping, and scissor lifts, where sparsity caused by occlusion and fragmented geometry make segmentation particularly challenging. The scanning protocol, annotation workflow, and quality control procedures establish a consistent foundation for the dataset. SIP is openly available with a supporting Git repository, offering adaptable class configurations that streamline adoption within modern 3D deep learning frameworks. By providing field data that retain real-world sensing characteristics, SIP enables robust benchmarking and contributes to advancing construction-oriented 3D vision tasks.

**Keywords:** Construction Lidar Dataset, 3D Point Cloud, Semantic Segmentation, Digital Twins

## INTRODUCTION

### Background: 3D Scene Understanding in Construction

3D scene understanding has become a foundational capability in modern construction engineering, driven by the increasing integration of digital technologies into field workflows (Chen et al. 2022). Over the past decade, construction projects have increasingly adopted terrestrial laser scanning (TLS) (Qin et al. 2021; Wang and Cho 2015), photogrammetry (Sestras et al. 2025), and other spatial sensing systems to support progress monitoring (Puri and Turkan 2020), safety assessment, quality assurance/quality control (Xu et al. 2019), as-built documentation (Sepasgozar and Shirowzhan 2016), and the development of digital twins (Liu et al. 2021; Wang et al. 2015).

Among these sensing modalities, LiDAR has become particularly prominent because it provides geometry-first measurements that remain reliable in cluttered, partially lit, and dynamically changing jobsite conditions. Unlike camera-based systems, whose performance can degrade under uneven illumination, repetitive textures, or occlusion, LiDAR consistently captures accurate spatial structure even when visual appearance is insufficient for reconstruction (Zhong et al. 2021). As a result, many construction workflows increasingly depend on LiDAR as their primary source of spatial information, shifting the focus toward extracting semantic meaning directly from LiDAR-derived point clouds. Consequently, the ability to interpret raw 3D point clouds has become essential for automated analysis, robotics, and information modeling in active construction environments (Wu et al. 2021).

However, construction environments introduce unique complexities that pose challenges radically different from those seen in conventional curated datasets used in 3D perception research (Chen et al. 2019; Park and Cho 2022). Construction sites are inherently dynamic, with structures evolving day by day as new materials are added, temporary installations are erected, and equipment and workers move throughout the space. They are also unstructured and cluttered, with a mixture of permanent components (e.g., walls, floors, columns), temporary systems (e.g., formwork, scaffolding, pipe frames), dynamic objects (e.g., equipment, workers) and miscellaneous items such as debris and tools. These conditions impose a level of geometric and semantic variability rarely represented in existing structured datasets.

Semantic segmentation of point clouds (i.e., assigning class labels to individual points) plays a critical role in making sense of such complex and dynamic environments. Segmentation outputs provide

the basis for object detection, progress quantification, hazard identification, robotic navigation, inspection workflows, and automated comparisons between as-designed and as-built models (Nguyen et al. 2020; Zhang et al. 2019; Zhao et al. 2019).

Yet, construction-phase data fundamentally differ from widely used benchmark datasets in several fundamental ways. 1) First, *on-site dynamics* create persistent occlusion and visual clutter. Equipment, workers, stored materials, and temporary assemblies frequently obstruct the scanner's view, and irregular spatial arrangement introduce overlapping geometry and mission regions that complicate semantic interpretation. 2) *Temporal evolution* continuously alters the environment. As work progresses, objects appear, disappear, or change configuration, and visibility conditions shift across scans. Because construction spaces seldom follow repetitive spatial patterns, these time-dependent changes limit the generalizability of models trained on more structured datasets. 3) Construction scenes often exhibit *High intra-class variability and low inter-class variability*. Objects within the same category may differ widely in shape or configuration, while components from different categories can share similar geometric characteristics, blurring class boundaries and complicate semantic discrimination.

Together, these characteristics highlight an unmet need for datasets that accurately reflect the realistic sensing conditions encountered during construction.

### **Practical Constraint: Single-scan or Partially Registered Field Data**

Despite recent progress in automated registration, construction sites rarely allow practitioners to capture comprehensive, multi-view reconstructions. In practice, field constraints frequently force the use of single-scan or only partially registered scans (Aryan et al. 2021). A single-scan denotes an isolated single-station LiDAR acquisition, resulting in a self-contained but inherently partial view of the scene. A partially registered scan refers to a small cluster of locally aligned scans, typically within a limited work zone.

Scanner placement is often limited by safety requirements around active work areas, and operators must avoid disrupting ongoing workflows, which restricts opportunities to revisit or refine viewpoints. Physical obstructions such as partitions, equipment, temporary installations, and accumulated materials

further prevent ideal positioning, while tight daily schedules encourage rapid and opportunistic data capture rather than deliberate multi-position planning.

Consequently, LiDAR data collected on real job sites rarely resemble the fully registered and geometrically complete models commonly used in research datasets. Instead, they consistently exhibit:

- *Radiating scan geometry* reflects the limited angular coverage of TLS, where visibility decreases with distance. Nearby surfaces are captured from broader viewing angles, whereas distant regions fall outside many beam paths, resulting in increased portions of unobserved geometry.

- *Partial and fragmented surfaces* arise because many objects are only observed from a single vantage point. Structural components, temporary assemblies, and slender objects are often captured only on the sides facing the scanner, leaving large regions missing and producing fragmented or incomplete shapes.

- *Irregular sampling distribution (nonuniform density)* results from the angular sampling structure of TLS. Sampling is disproportionately concentrated near the scanner, while surfaces that are angled, recessed, or farther away receive fewer measurements. This results in uneven point distributions across the scene, independent of the visibility limitations described earlier.

- *Unregistered partial scenes* arise because multiple scans are rarely merged into full-scene reconstructions during field operations. Each scan remains an independent capture containing only the geometry visible from its specific position, resulting in partial rather than consolidated site representations.

These sensing artifacts are not merely imperfections but intrinsic outcomes of terrestrial laser scanning under real jobsite conditions, and therefore constitute the predominant form of LiDAR data encountered in practice. Even in this incomplete state, single-scan measurements still contain meaningful information for construction 3D vision tasks. The ability to interpret single-scan observations enables field-collected data to be used directly, without requiring additional acquisition passes or rework. These considerations motivate the need for datasets that capture the practical sensing conditions during construction.

## **Landscape of Public 3D Datasets for Deep Learning**

While the computer vision and robotics communities have produced several influential 3D datasets, none capture the sensing conditions characteristic of construction-phase scanning. Popular indoor datasets such as S3DIS (Armeni et al. 2016), ScanNet (Dai et al. 2017), and Matterport3D (Chang et al. 2017) provide high-quality, multi-view reconstructions of clean, structured spaces such as offices, homes, and public buildings. These datasets generally reflect clean, stable indoor environments with broad visibility and well-structured spatial layouts.

Outdoor datasets, including SemanticKITTI (Behley et al. 2021), Semantic3D (Hackel et al. 2017), and DALES (Varney et al. 2020), focus on autonomous driving or aerial mapping. Their sensor perspectives, object categories, and geometric characteristics differ significantly from those encountered in indoor construction settings. For example, driving datasets exhibit consistent radial patterns and contain vehicle- or street-related classes, whereas construction sites require recognition of frames, scaffolds, formwork, and equipment rarely found in these sources.

Synthetic datasets such as ShapeNet (Chang et al. 2015), Objaverse (Deitke et al. 2023), or large-scale graphics-generated repositories offer complete, perfectly sampled geometry with clean object boundaries. While valuable for shape understanding, they do not replicate LiDAR occlusion, cluttered arrangements, or density decay, limiting their suitability for real-world representation. Dynamic datasets such as NSS (Sun et al. 2023) document multi-phase construction changes using multi-view RGB imagery and derived depth to generate 3D reconstructions. They provide complete multi-view visibility across phases and offer detailed observations of evolving structural conditions.

A comparative review of public 3D datasets (see Table 1) shows that their underlying sensing assumptions differ markedly from the realities of construction-phase data. Most existing datasets are collected in stable environments with consistent viewpoints and near-complete geometric coverage. Visibility patterns are predictable, scenes remain largely unchanged during acquisition, and object compositions are typically well structured. These differences highlight a broader landscape gap: while many high-quality 3D datasets exist, few reflect environments where incomplete geometry, evolving visibility, and diverse object compositions are fundamental characteristics of the data that are intrinsic to construction-specific environments.

**Table 1.** Comparison of public 3D datasets used in 3D perception research.

Dataset	Domain Description	Acquisition Modality	Visibility
<i>S3DIS</i>	<ul style="list-style-type: none"> <li>Indoor; office-like; minimal clutter</li> </ul>	TLS	<ul style="list-style-type: none"> <li>Multi-view, complete or near-complete visibility</li> </ul>
<i>ScanNet</i>	<ul style="list-style-type: none"> <li>Indoor; consumer/residential; curated</li> </ul>	RGB-D	<ul style="list-style-type: none"> <li>Multi-view reconstructed; mostly complete with partial occlusion</li> </ul>
<i>Matterport3D</i>	<ul style="list-style-type: none"> <li>Indoor; real-estate style environments</li> </ul>	RGB-D	<ul style="list-style-type: none"> <li>Panoramic registered views; complete visibility</li> </ul>
<i>SemanticKITTI</i>	<ul style="list-style-type: none"> <li>Outdoor driving; vehicle-centric</li> </ul>	64-beam LiDAR	<ul style="list-style-type: none"> <li>Sequential driving viewpoint; sparse object visibility and partial silhouettes</li> </ul>
<i>Semantic3D</i>	<ul style="list-style-type: none"> <li>Outdoor static; urban plazas</li> </ul>	TLS	<ul style="list-style-type: none"> <li>Fully registered static scans; very complete with minimal occlusion</li> </ul>
<i>DALES</i>	<ul style="list-style-type: none"> <li>Aerial; rooftops and terrain</li> </ul>	ALS	<ul style="list-style-type: none"> <li>Top-down coverage; limited side-geometry visibility</li> </ul>
<i>Objaverse</i>	<ul style="list-style-type: none"> <li>Synthetic; complete 3D assets</li> </ul>	Synthetic	<ul style="list-style-type: none"> <li>Fully visible synthetic geometry; no occlusion</li> </ul>
<i>NSS</i>	<ul style="list-style-type: none"> <li>Construction-specific dynamic scenes; multi-phase change capture</li> </ul>	Multi-view stereo	<ul style="list-style-type: none"> <li>Dynamic temporal changes; Multi-view captures with complete visibility</li> </ul>
<i>SIP (Ours)</i>	<ul style="list-style-type: none"> <li>Construction-phase; realistic jobsite scan conditions</li> </ul>	TLS	<ul style="list-style-type: none"> <li>Single-viewpoint captures; severely occluded, incomplete partial-view</li> </ul>

### Distinctive Contributions of the SIP Dataset

To bridge this gap, we introduce SIP (Sites in Pieces), a dataset designed to capture construction-phase point clouds in the form in which they are realistically acquired in the field. SIP consists of disaggregated, individual terrestrial LiDAR scans collected using a Faro TLS, preserving the raw characteristics intrinsic to jobsite scanning, including partial visibility, limited viewpoint coverage, and sampling inconsistencies.

The dataset encompasses a diverse range of construction elements, covering both permanent components (such as ceilings, floors, columns, and partitions) and temporary or slender objects (including pipes, ladders, guardrails, material piles, and other transient assemblies). All scans are annotated at the point level following a structured taxonomy tailored to construction environments. SIP dataset supports several emerging research needs in construction-oriented 3D perception, including

segmentation under partial observation, density-aware and distance-aware learning strategies, robotic perception for navigation and human–robot interaction, and the development of generalizable models suitable for real-world deployment.

The key contributions of SIP can be summarized as follows:

- A realistic construction-phase 3D dataset, capturing isolated single-scan LiDAR scenes that preserve occlusion, incompleteness, density imbalance, and other sensing constraints inherent to jobsite conditions.
- A comprehensive construction-specific semantic annotation set, covering both permanent structures and slender temporary construction objects often missing from existing datasets.
- A reusable dataset infrastructure, including class configuration files, metadata, and visualization utilities to support reproducibility and ease of integration into common 3D perception frameworks.
- Support for advanced research directions, enabling studies on occlusion-robust segmentation, density-adaptive learning, construction robotics perception, and automated digital twin generation.

Together, these contributions enable researchers and practitioners to develop and evaluate 3D perception methods that operate robustly under the genuine constraints of active construction sites.

## **DATASET DESCRIPTION**

### **Dataset Philosophy and Acquisition Context**

The SIP dataset is designed to advance 3D scene understanding and semantic segmentation in construction environments by emphasizing single-scan realism and construction-phase complexity. Each scan originates directly from TLS acquisition without global alignment or multi-scan fusion, preserving the inherent geometric irregularities, occlusions, and density gradients that characterize real construction sensing. This acquisition philosophy reflects how segmentation models must operate in practice on incomplete, partially occluded scenes, where object visibility is highly dependent on scanner placement and ongoing construction activities, as illustrated in Figure 1. Instead of smoothing or correcting these properties, SIP deliberately retains them to facilitate research addressing uneven point

data distribution, variable visibility, and geometric uncertainty.

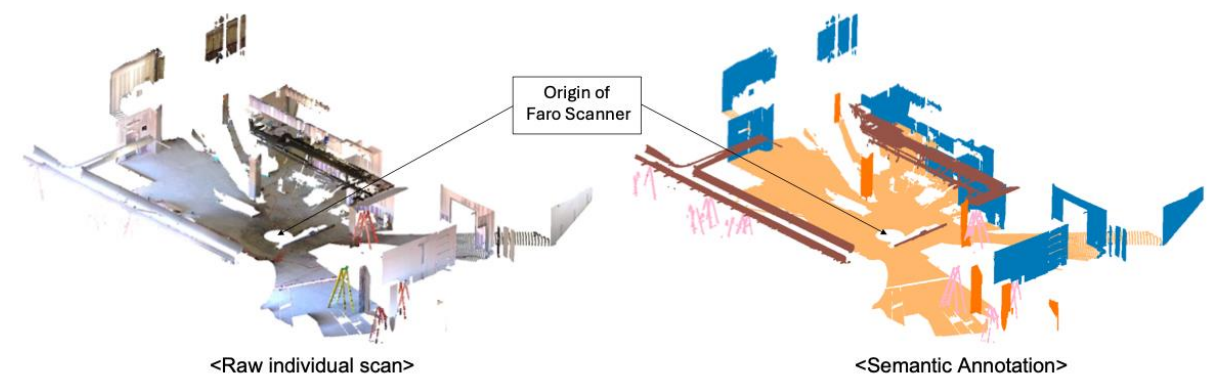


**Fig. 1.** Illustration from the SIP dataset demonstrating single-scan LiDAR acquisition. The raw scan (left) and semantic annotation (right) highlight clutter, occlusion, the scanner origin, and the radial spread pattern of outward-propagating LiDAR returns.

SIP consists of 40 single-scan LiDAR scenes, including 27 indoor and 13 outdoor environments. Each scan contains on average 3–5 million points, and the dataset provides 23 semantic classes representing structural elements, temporary construction objects, and site-context features.

### Composition of SIP Scenes and Dataset

This section provides an overview of the SIP dataset, summarizing its overall composition and detailing the indoor and outdoor scenes that collectively represent the full dataset.

#### *Dataset Overview*

SIP captures diverse indoor and outdoor construction environments through isolated single-station LiDAR acquisitions. Across all scenes, the dataset reflects the visual and geometric conditions of active jobsites, where partially completed structures, exposed systems, temporary equipment, and ongoing operations produce irregular and evolving spatial configurations (Figure 2). These conditions lead to cluttered layouts, shifting material arrangements, and heterogeneous surface properties, collectively contributing to the realism and variability that characterize SIP scans.



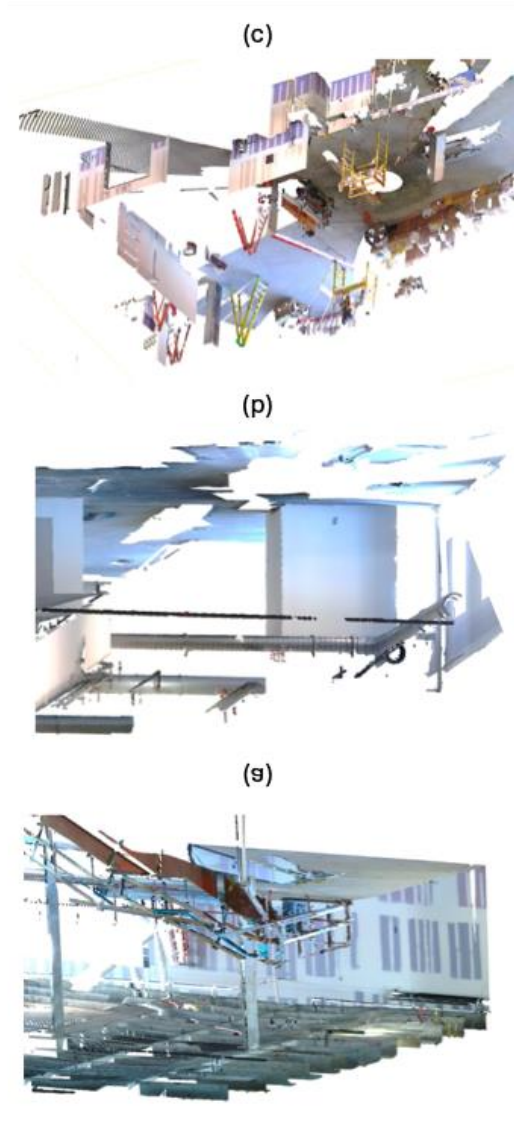


**Fig. 2.** Representative construction-phase elements captured in SIP scans: (a) stair structures in the midst of framing, (b) exposed mechanical and piping systems prior to enclosure, and (c) temporary construction equipment including ladders, lifts, and materials.

In addition to construction-phase complexity, the dataset also preserves the natural sensing behavior inherent to terrestrial LiDAR acquisition. As shown in Figure 3, SIP scans exhibit a clear center-weighted point distribution that reflects the radial density imbalance inherent to single-scan acquisition. Combined with occlusions caused by structural elements and limitations on scanner placement, this results in incomplete geometry and restricted visibility. The highly uneven point density across each scene further presents challenges for deep learning models to learn from inconsistent sampling patterns. Together, these effects create the distinctive data profiles of SIP.

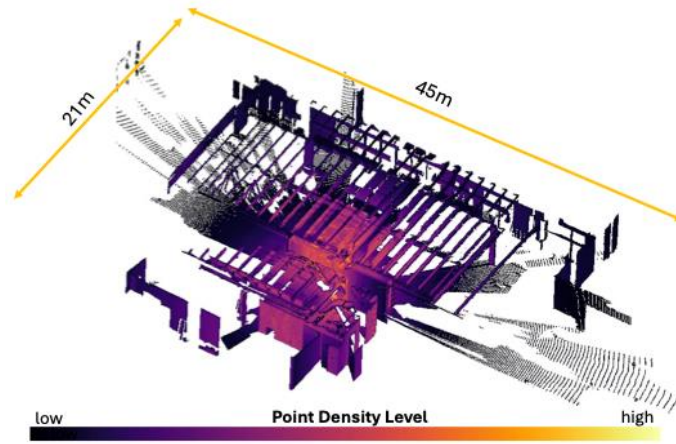


**Fig. 3.** SIP point-density map showing strong central point concentration (half within 5 m radius) across a scene spanning approximately 21 m  $\times$  45 m.

SIP also spans a wide range of spatial footprints, from compact rooms to large open interiors and exterior site environments. This diversity leads to substantial variation in point counts across scenes. Each indoor scan averages approximately 3 million points, while each outdoor scan averages approximately 5 million points, reflecting the broader, more variable coverage typical of exterior construction environments (Figure 4). These variations in scale, density, and scene structure provide a meaningful basis for evaluating how segmentation and perception methods generalize across contrasting construction conditions.

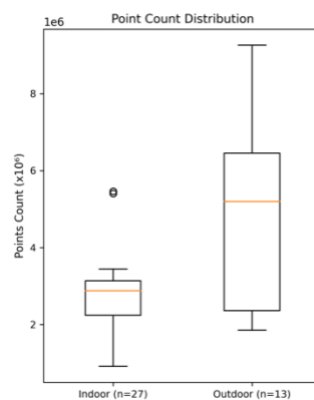


**Fig. 4.** Per-scan point count distribution for indoor and outdoor SIP scenes, showing the larger variation and higher overall point counts present in outdoor scans.

### *Indoor Scene Composition*

Indoor scenes in SIP represent a variety of construction phase interior spaces, including open halls, compact enclosures, linear corridors, and stairwells (Table 2). These environments can be broadly described in terms of four spatial patterns that reflect the geometric constraints common to active construction. Open halls offer wide visibility and expansive floor areas; enclosures form tight bounded volumes; corridors create narrow elongated pathways; and stairwells introduce vertical circulation with inherent occlusion, as shown in Figure 5. These spatial patterns illustrate the diversity of interior settings encountered during scanning and provide contextual understanding of the indoor scenes represented in the dataset.

**Table 2.** Indoor SIP scan distribution by spatial pattern and variant.

Category (with variant)	Scan count	Subtotal
Open Hall	—	20
Core	15	
w/ staircase	3	
w/ enclosure	1	
w/ corridor	1	
Enclosure	—	5
Core	3	
w/ corridor	2	
Corridor	1	1
Stairwell	1	1
		27

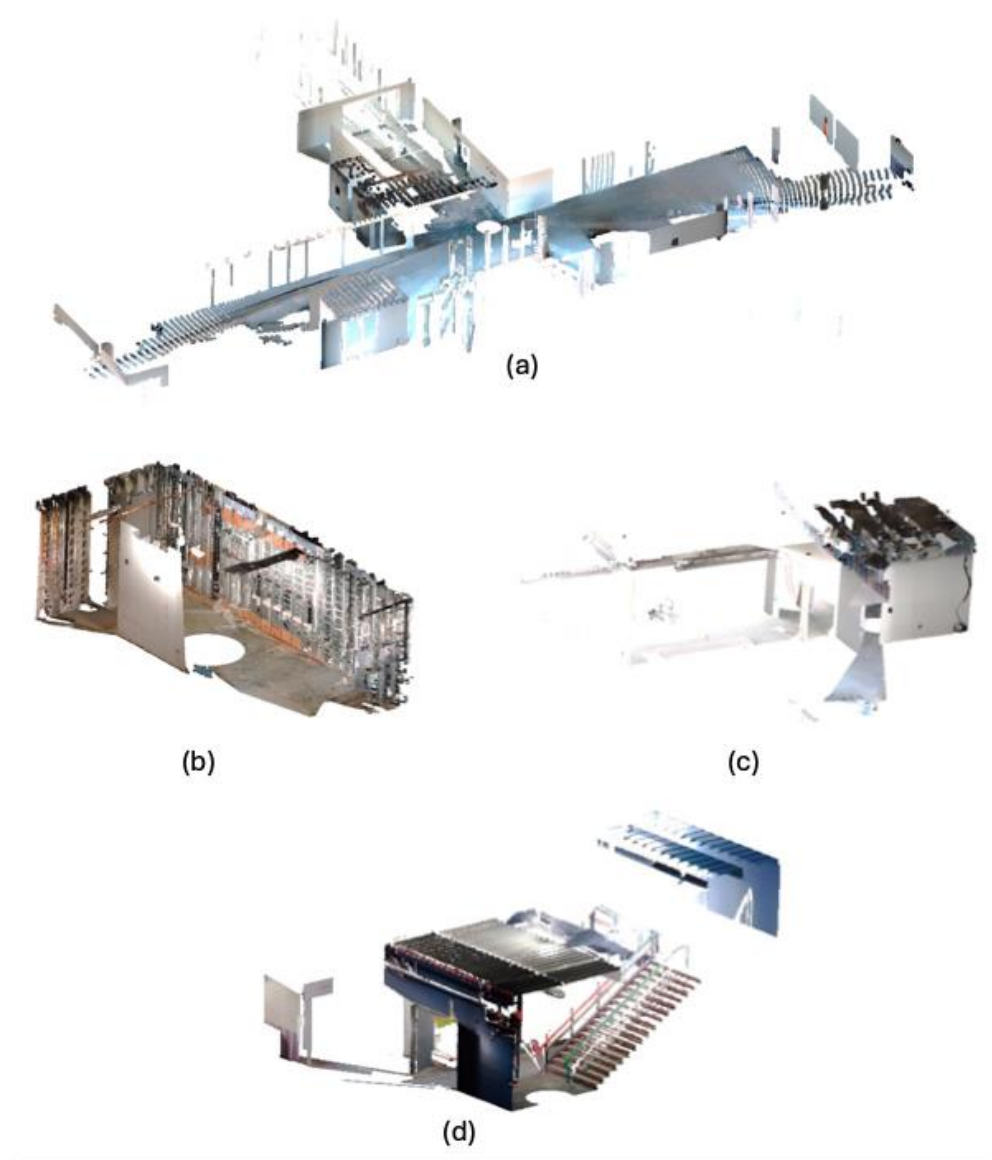


**Fig. 5.** Representative indoor scan examples illustrating four spatial patterns: (a) open interior volumes, (b) enclosed rooms, (c) corridors, and (d) stairwells.

Across these interiors, partially completed structural elements, such as walls, ceilings, floors, and columns, form the primary geometry, while exposed MEP systems such as ducts, conduits, and piping reflect ongoing construction work. Temporary items, including ladders, scissor lifts, opening frames, scaffolding components, and stored materials, frequently appear in the scans, introducing clutter and irregular object arrangements.

Indoor scanning conditions also shape the data. Shorter distances between the scanner and surrounding surfaces produce higher point density and more complete geometry than outdoor

environments. Because indoor spaces are often bounded by ceilings and surrounding walls, a larger portion of the full 360-degree view is captured as meaningful geometry, with fewer empty regions and less wasted scan coverage.

#### *Outdoor Scene Composition*

Outdoor scenes in SIP capture the broader and less structured settings of active construction sites. These scans encompass open work areas, site perimeters, staging zones, and exterior building surroundings, each shaped by variable terrain, larger spatial extents, and constantly changing operational conditions. A representative sample of outdoor scans is shown in Figure 6.

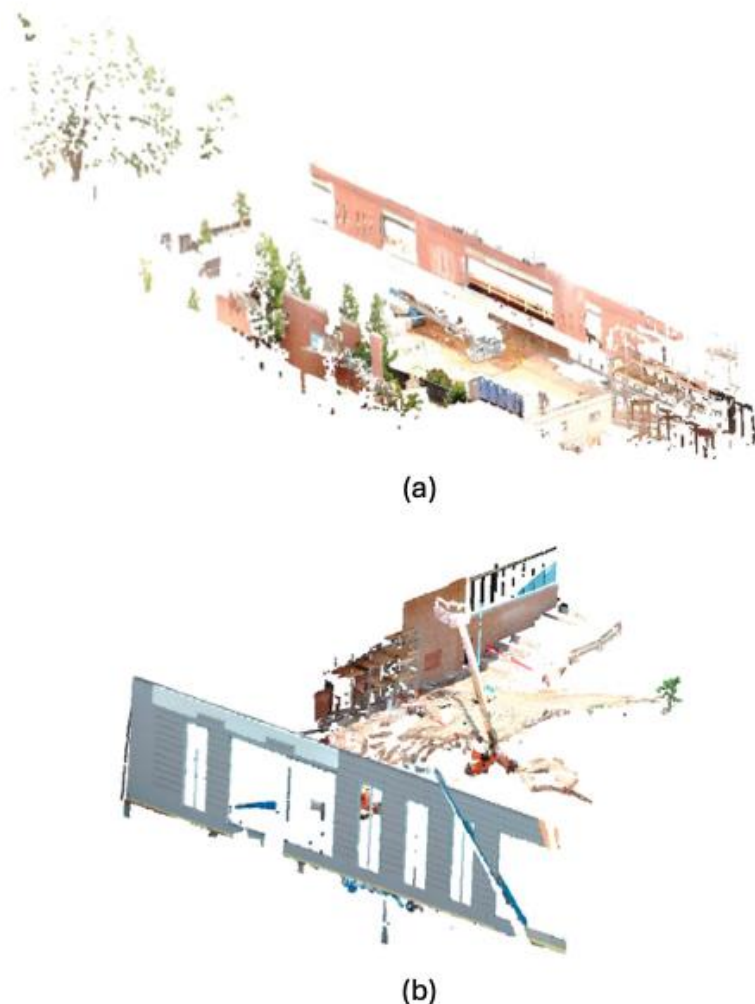


**Fig. 6.** Representative outdoor scans showing exterior construction elements, including ground surfaces, vehicles, fencing, scaffolding, and temporary site infrastructure: (a) façade view; (b) similar exterior view with additional site equipment.

Unlike indoor environments, outdoor scenes lack the enclosing boundaries that constrain visibility and geometry. As a result, they exhibit wide, sparse point distributions and substantial variability in coverage. Ground surfaces, vegetation, temporary fencing, vehicles, and site logistics elements commonly appear, reflecting the diverse exterior conditions encountered during construction.

Outdoor scans also present more complex sensing challenges. Heavy equipment, stored materials, and site layout constraints introduce irregular occlusions, while dynamic activities, such as moving workers, vehicles, or machinery, can produce transient artifacts. Natural lighting, weather exposure, and surface reflectivity variation further influence the appearance and distribution of LiDAR returns. This diversity makes outdoor scans particularly valuable for studying perception robustness under fluctuating environmental conditions, though they also introduce long-tail object classes and sparse sampling that may challenge segmentation and recognition models.

### **Point Cloud Attribute Schema**

Each SIP scan is stored as a point cloud in a simple, platform-independent text format, with each point containing 1) spatial coordinates, 2) color values, 3) return intensity, and 4) a surface normal. This straightforward structure allows the data to be easily parsed, visualized, and used for algorithm development without reliance on proprietary formats.

The spatial coordinates (XYZ) represent the 3D position of each point in meters and form the geometric backbone of the scans. Color values (RGB), stored as integers in the 0 to 255 range, provide appearance cues that help distinguish materials and surface conditions in construction environments. Intensity values are also stored as integers in the 0 to 255 range and indicate the relative strength of each LiDAR return rather than a calibrated radiometric measurement. FARO typically provides relative intensity values, and when exported in ASCII format these values fall within the same 0 to 255 range used in SIP. Surface normals capture local planar structure and orientation, and these dimensionless unit vectors offer additional geometric cues useful for segmentation, plane detection, and other spatial reasoning tasks.

Because raw terrestrial LiDAR scans contain millions of points, SIP applies a controlled down-

sampling step to make the data more suitable for 3D model training workflows. Uniform random sampling is performed after annotation to preserve the natural density imbalance of the original scans. The resulting point counts approximate those produced by voxel down-sampling at approximately 0.01 meters, a deliberately conservative resolution while allowing researchers to apply their own preferred downsampling strategies. This choice also maintains compatibility with the effective point resolutions (0.02–0.05 m) commonly used in public 3D segmentation datasets (Armeni et al. 2016; Chang et al. 2017; Dai et al. 2017).

### **Class Taxonomy**

SIP defines a total of 23 semantic classes, grouped into three functional categories that reflect their roles in construction settings. This taxonomy provides a clear and simple structure for interpreting objects across indoor and outdoor scenes while capturing the diversity of elements present in construction-phase environments (Table 3).

A. *Built Environment Elements*: Permanent or in-progress components of the built structure.

A1. Permanent Structural Components- 1) wall, 2) ceiling, 3) floor, 4) column, 5) stair framing, 6) girder

A2. In-Progress Built Components- 7) MEP piping, 8) opening framing, 9) window, 10) door, 11) awning

B. *Construction Operations Elements*: Elements that support construction activities, on-site operations, and the handling or movement of equipment and materials.

B1. Works & Access Structures- 12) guardrails, 13) site fence, 14) scaffolding

B2. Operational Equipment- 15) step ladder, 16) scissor lift

B3. Site Logistics- 17) staged materials, 18) porta john, 19) office trailer

C. *Site Surroundings*: Natural or site-context elements that are not part of the constructed facility - 20) ground, 21) tree, 22) monument, 23) vehicle

**Table 3.** SIP class applicability for indoor and outdoor scenes, organized by functional group

Class Group	Indoor	Outdoor
A. Built Environment		
A1. Permanent Structural	wall, ceiling, floor, column, stair framing, girder	wall, floor, girder, awning
A2. In-Progress Built	MEP piping, window, door, opening framing	window
B. Construction Operations		
B1. Access Structures	guardrails, site fence	guardrails, site fence, scaffolding
B2. Operational Equipment	step ladder, scissor lift	construction vehicle
B3. Site Logistics	staged materials	staged materials, office trailer, porta john
C. Site Surroundings	—	ground, tree, monument

## METHODOLOGY AND DATA COLLECTION

### Dataset Collection Protocol

All scans were collected using the FARO terrestrial laser scanner equipped with a dual-capture system that simultaneously records LiDAR geometry and 70-megapixel color imagery. The sensor provides a 300° vertical and full 360° horizontal field of view, using a Class 1 laser with a divergence of 0.19 mrad (0.011°). The angular sampling step is approximately 0.009° in both axes, and the manufacturer-specified ranging error is  $\pm 0.2$  mm when noise compression is disabled. Each scan required roughly 15 minutes to complete depending on resolution settings. To maintain consistency across scenes, the tripod height was kept around 1.4–1.5 meters.

Data were collected at the student center construction project on the Georgia Tech campus (Figure 7). The interior spaces were undergoing phased construction across three floors, while the exterior frontage hosted ongoing work involving equipment, materials, and active site traffic. A total 40 scanning was collected over a 5-month period during interior finishing operations such as drywall installation, pipe routing, mechanical work, and stair assembly, along with selected exterior activities.





**Fig. 7.** Aerial 3D reconstruction of the John Lewis Student Center site, including the active construction frontage, produced using drone-based photogrammetry.

Scan positions were intentionally selected for single-scan use rather than multi-scan registration. Each vantage point was chosen to maximize coverage from a single observation position, typically the center of a room, open lobby, or strategic corridor intersection. This approach preserved natural visibility limitations and resulted in scenes that realistically reflect occlusion, partial geometry, and nonuniform density. Indoor scenes generally provided clearer line-of-sight conditions, while outdoor scenes involved larger standoff distances, façade-level geometry, and increased variability. No registration or global alignment was performed so that each scan remained an independent representation of a construction state. Position choices also reflected practical constraints such as safety boundaries, obstructed paths, and worker movement near the scanner.

Site access was tightly constrained throughout the project, as active construction limited both the areas we were permitted to enter and the amount of time we could remain in each zone. In practice, this meant that only a subset of the site was reachable during any given visit, and even those areas were far from static or controllable. Scanning was therefore carried out during short windows, typically around lunch hours to reduce interference. Even then, the environment remained highly dynamic due to constant worker movement and shifting site conditions.

These practical constraints naturally shaped the acquisition strategy. Rather than attempting comprehensive multi-scan coverage, the approach focused on obtaining the maximum observable

geometry from single, strategically positioned scans in each accessible space. This constraint-driven methodology is foundational to the SIP dataset, where each scan quickly captures a realistic, partial view of an active construction scene under real operational limitations.

### **Annotation Procedure**

Raw point measurements were collected in the proprietary FARO.fls format, which was later converted into plain ASCII .txt files containing XYZ coordinates, RGB values, intensity, and surface normals. Normals were computed using the Open3D library when they were not present in the exported files. No downsampling, smoothing, or filtering beyond basic noise removal was applied in order to preserve the raw characteristics of single-scan LiDAR geometry.

CloudCompare (CloudCompare 2025) was used as an annotation tool. Annotators used simple editing utilities such as rectangular and polygonal selection, along with connectivity-based extraction for object-specific segmentation. No automated or color-based segmentation modules were used to ensure that all labels reflect deliberate human interpretation.

Annotation began with manual removal of isolated noise, ghost points, and small clusters that did not represent physical surfaces. After denoising, annotators segmented each class individually, resulting in per-class files aligned with the SIP dataset structure. Three trained annotators, each with field experience in construction, followed a shared labeling guideline to maintain consistency. Only visible geometry was labeled; occluded surfaces were not inferred or completed. All labeled scans were cross-checked before inclusion in the final dataset to ensure correctness and adherence to class definitions.

### **DATA VALIDATION AND QUALITY CONTROL**

This section summarizes how the SIP dataset was validated for spatial plausibility, annotation correctness, and consistent formatting. Because SIP is composed of single, vantage-point-dependent scans captured in an active construction site, validation focuses on internal coherence rather than global completeness. The validation workflow progresses from raw scan export to annotation checks, scene-

level plausibility review, and final dataset-wide consistency enforcement. Automated scripts detect missing attributes, malformed files, or unusually sparse classes, ensuring uniform standards across all scans.

### **Validation Rationale**

Single-scan construction data inherently include occlusion, uneven density, and limited visibility, making completeness-based validation infeasible. Validation instead ensures that each scan plausibly reflects the visible scene, maintains geometric coherence, and preserves natural field conditions without over-cleaning or reconstructing unseen regions.

### **Annotation and Scene-Level Quality Control**

Annotation quality control combined iterative manual review with structured cross-verification among trained annotators. Each class was inspected to confirm boundary precision, proper adherence to class definitions, and consistent treatment of slender, reflective, or partially occluded elements such as pipes, conduits, and temporary supports. Annotators referenced a shared guideline, and any disagreements were resolved through short review sessions led by a senior annotator to maintain uniform interpretation across the dataset.

Scene-level validation ensured that annotations were both geometrically and contextually plausible. Labels were verified against the cleaned scan to confirm a one-to-one match with visible surfaces, and any overlapping or duplicate labels were corrected. Additional plausibility checks examined whether architectural elements exhibited expected geometric behavior, for example, walls remaining planar, floors maintaining consistent elevation, and structural elements showing realistic verticality. Color-geometry alignment was reviewed to detect potential RGB misregistration, and all major visible components were confirmed to be fully annotated without omissions. This combined procedure ensured that each annotated scene was coherent, complete with respect to visible geometry, and free from labeling conflicts.

### **Dataset-Wide Consistency Checks**

Dataset-wide checks enforced consistent directory structure, class mapping, and annotation formatting

across all indoor and outdoor scans. Automated scripts verified that each scene contained the complete set of point attributes, such as, XYZ coordinates, RGB color values, LiDAR intensity, and surface normals, and that all numeric ranges were physically valid. Additional integrity checks detected malformed files, missing attributes, or annotation folders containing empty or unintentionally sparse classes.

To ensure privacy and uniformity, all scan folders were anonymized using UUID-based identifiers during final packaging, replacing any site- or time-specific naming inherited from the field acquisition phase. Cross-scene consistency was also reviewed by comparing class-frequency patterns to identify outliers or mislabeled categories.

Note that no human-subject data or personally identifiable information is included in the dataset. Scenes occasionally contain workers or moving objects, but LiDAR returns are too sparse to reveal identity, and no RGB imagery of people was retained.

A representative figure showing the original, intensity, normal, and annotation panels is included to support misalignment inspection (Figure 8). Viewing these channels side-by-side helps reveal issues such as RGB–geometry drift, inconsistencies in normal orientation, or annotation boundaries that deviate from geometric or radiometric cues. This visual comparison provides a direct, intuitive way to confirm annotation correctness and overall file integrity.

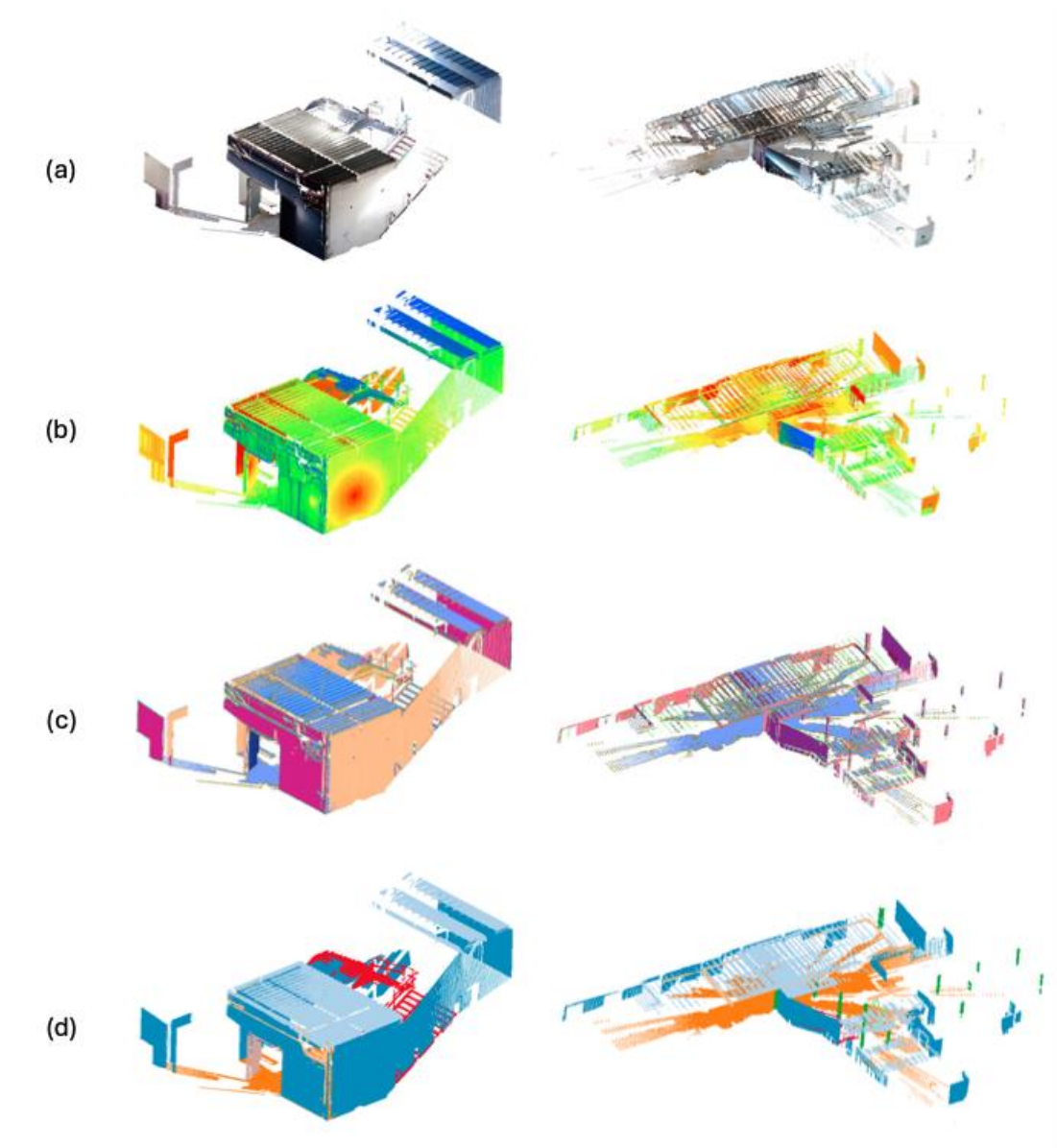


**Fig. 8.** Multi-attribute visualization for misalignment and annotation verification. (a) RGB rendering, (b) LiDAR intensity, (c) normal orientation, and (d) final semantic labels.

## USAGE NOTES

### Dataset Usage

The SIP dataset is openly accessible through its DOI (<https://doi.org/10.5281/zenodo.17667736>), ensuring long-term availability, while all utility scripts and usage instructions are maintained in the accompanying GitHub repository ([https://github.com/syoi92/SIP\\_dataset](https://github.com/syoi92/SIP_dataset)), with a stable version

archived under the dataset DOI. The dataset is released under the CC BY-NC 4.0 license, and the code is distributed under the MIT license to support transparent reuse and adaptation.

Each scan folder follows a consistent directory structure, illustrated in Figure 9. The ‘*scans/*’ directory contains the down-sampled single-scan point clouds in ASCII .txt format, whereas the ‘*Annotation/*’ directory stores per-class annotation files corresponding to the same scan. The file ‘*class\_config.json*’ contains class labels, associated RGB color codes for visualization, and an index flag indicating which classes are intended for training or evaluation. Dataset partitions are provided in ‘*splits.json*’, which maps each scan to the train, validation, or test split.

```
sip-indoor/  
├── class_config.json  
├── splits.json  
└── scans/  
    ├── scan.txt [xyzrgbINor] - original scan (pre-annotation)  
    └── Annotation/  
        ├── class1.txt [xyzrgbINor]  
        ├── class2.txt  
        ├── ...  
        └── classN.txt
```

**Fig. 9.** Directory structure of the SIP-Indoor dataset

Two helper scripts are included for practical use.

- `view_anno.py` produces class-wise color-coded point clouds by combining the raw scan with its annotation files according to the color definitions in `class_config.json`. This allows users to verify annotation quality and examine scene composition in any standard point-cloud visualization tool.
- `preprocessing.py` supports model-training workflows by reading the class indices from `class_config.json` and the dataset partitions from `splits.json`. It generates train, validation, and test sets containing only the selected classes and outputs dictionary-style tensors including coordinates, RGB values, intensity, normals, and class labels. Importantly, to preserve realistic acquisition characteristics, preprocessing also reorders points to approximate the original LiDAR scanning pattern.

## Model Training Pipeline

The dataset is designed to support contemporary 3D perception models such as PointCept (Pointcept Contributors 2023), MinkowskiEngine (Choy et al. 2019), Point Transformer (Wu et al. 2022, 2024; Zhao et al. 2021), and sparse convolutional backbones (Çiçek et al. 2016).

However, in practice, not all annotated classes are equally suitable for training. Construction environments contain many small, rare, or partially occluded objects, and deep learning models struggle to learn reliable representations for every category. Thus, we propose using a recommended subset of indexed classes for SIP-Indoor baseline experiments. These include wall, ceiling, floor, pipes, column, ladder, and stair—objects that appear consistently and exhibit stable geometry across scenes. The remaining categories are retained as auxiliary or extended classes, enabling research on robustness, long-tail distributions, or future expansion beyond indoor environments.

Users may flexibly modify which classes are included in training by editing the class configuration. The preprocessing script automatically incorporates this selection, producing training datasets aligned with the user’s chosen experimental setup. A typical workflow is as follows:

1. Examine the raw scan and its annotation files using 3D tools;
2. Update `class_config.json` to define the desired training classes;
3. Run preprocessing to generate train, validation, and test sets in dictionary format; and
4. Convert these outputs as needed to match the input requirements of the target 3D deep learning framework.

## CONCLUSION

The SIP dataset provides construction-phase TLS scans with realistic occlusion, incomplete visibility, and rich annotations for semantic segmentation and scene understanding. By releasing SIP and its supporting metadata and utilities, we aim to support research in construction automation, robust 3D perception, and benchmarking under practical jobsite conditions. Future extensions will include expanded scenes and accompanying model benchmarks.

## DATA AVAILABILITY STATEMENT

The SIP dataset introduced in this paper is openly available in a permanent, DOI-assigned repository. The full dataset, including raw LiDAR scans, point-level annotations, and metadata files, can be accessed at: <https://doi.org/10.5281/zenodo.17667736>. The dataset is licensed under CC BY-NC 4.0, allowing non-commercial reuse with proper attribution.

## REFERENCE

- Armeni, I., O. Sener, A. R. Zamir, H. Jiang, I. Brilakis, M. Fischer, and S. Savarese. 2016. “3D semantic parsing of large-scale indoor spaces.” *Proceedings of the IEEE Computer Society Conference on Computer Vision and Pattern Recognition*, 2016-Decem: 1534–1543. <https://doi.org/10.1109/CVPR.2016.170>.
- Aryan, A., F. Bosché, and P. Tang. 2021. “Planning for terrestrial laser scanning in construction: A review.” *Automation in Construction*, 125: 103551. Elsevier.
- Behley, J., M. Garbade, A. Milioto, J. Quenzel, S. Behnke, J. Gall, and C. Stachniss. 2021. “Towards 3D LiDAR-based semantic scene understanding of 3D point cloud sequences: The SemanticKITTI Dataset.” *The International Journal of Robotics Research*, 40 (8–9): 959–967. SAGE Publications Sage UK: London, England.
- Chang, A., A. Dai, T. Funkhouser, M. Halber, M. Niessner, M. Savva, S. Song, A. Zeng, and Y. Zhang. 2017. “Matterport3d: Learning from rgb-d data in indoor environments.” *arXiv preprint arXiv:1709.06158*.
- Chang, A. X., T. Funkhouser, L. Guibas, P. Hanrahan, Q. Huang, Z. Li, S. Savarese, M. Savva, S. Song, and H. Su. 2015. “Shapenet: An information-rich 3d model repository.” *arXiv preprint arXiv:1512.03012*.
- Chen, J., Y. K. Cho, and Z. Kira. 2019. “Multi-View Incremental Segmentation of 3-D Point Clouds for Mobile Robots.” *IEEE Robotics and Automation Letters*, 4 (2): 1240–1246. <https://doi.org/10.1109/LRA.2019.2894915>.



- Chen, X., A. Y. Chang-Richards, A. Pelosi, Y. Jia, X. Shen, M. K. Siddiqui, and N. Yang. 2022. "Implementation of technologies in the construction industry: a systematic review." *Engineering, Construction and Architectural Management*, 29 (8): 3181–3209. Emerald Publishing Limited.
- Choy, C., J. Gwak, and S. Savarese. 2019. "4d spatio-temporal convnets: Minkowski convolutional neural networks." In: *Proceedings of the IEEE/CVF conference on computer vision and pattern recognition*, 3075–3084.
- Çiçek, Ö., A. Abdulkadir, S. S. Lienkamp, T. Brox, and O. Ronneberger. 2016. "3D U-Net: learning dense volumetric segmentation from sparse annotation." In: *International conference on medical image computing and computer-assisted intervention*, 424–432. Springer.
- CloudCompare. 2025. "3D point cloud and mesh processing software Open Source Project." Accessed December 7, 2025. <https://www.cloudcompare.org/>.
- Pointcept Contributors. 2023. "Pointcept: A codebase for point cloud perception research." Accessed December 7, 2025. <https://github.com/Pointcept/Pointcept>.
- Dai, A., A. X. Chang, M. Savva, M. Halber, T. Funkhouser, and M. Nießner. 2017. "ScanNet: Richly-annotated 3d reconstructions of indoor scenes." In: *Proceedings of the IEEE conference on computer vision and pattern recognition*, 5828–5839.
- Deitke, M., D. Schwenk, J. Salvador, L. Weihs, O. Michel, E. VanderBilt, L. Schmidt, K. Ehsani, A. Kembhavi, and A. Farhadi. 2023. "Objaverse: A universe of annotated 3d objects." In: *Proceedings of the IEEE/CVF conference on computer vision and pattern recognition*, 13142–13153.
- Hackel, T., N. Savinov, L. Ladicky, J. D. Wegner, K. Schindler, and M. Pollefeys. 2017. "Semantic3d. net: A new large-scale point cloud classification benchmark." *arXiv preprint arXiv:1704.03847*.
- Liu, J., D. Xu, J. Hyppä, and Y. Liang. 2021. "A survey of applications with combined BIM and 3D laser scanning in the life cycle of buildings." *IEEE Journal of Selected Topics in Applied Earth*

*Observations and Remote Sensing*, 14: 5627–5637. IEEE.

Nguyen, T. A., P. T. Nguyen, and S. T. Do. 2020. “Application of BIM and 3D laser scanning for quantity management in construction projects.” *Advances in Civil Engineering*, 2020 (1): 8839923. Wiley Online Library.

Park, J., and Y. K. Cho. 2022. “Point Cloud Information Modeling: Deep Learning–Based Automated Information Modeling Framework for Point Cloud Data.” *Journal of Construction Engineering and Management*, 148 (2): 4021191. American Society of Civil Engineers.

Puri, N., and Y. Turkan. 2020. “Bridge construction progress monitoring using lidar and 4D design models.” *Automation in Construction*, 109: 102961. Elsevier.

Qin, G., Y. Zhou, K. Hu, D. Han, and C. Ying. 2021. “Automated reconstruction of parametric BIM for bridge based on terrestrial laser scanning data.” *Advances in Civil Engineering*, 2021 (1): 8899323. Wiley Online Library.

Sepasgozar, S. M. E., and S. Shirowzhan. 2016. “Challenges and opportunities for implementation of laser scanners in building construction.” In: *ISARC. Proceedings of the international symposium on automation and robotics in construction*, 1. IAARC Publications.

Sestras, P., G. Badea, A. C. Badea, T. Salagean, S. Roşca, S. Kader, and F. Remondino. 2025. “Land surveying with UAV photogrammetry and LiDAR for optimal building planning.” *Automation in Construction*, 173: 106092. Elsevier.

Sun, T., Y. Hao, S. Huang, S. Savarese, K. Schindler, M. Pollefeys, and I. Armeni. 2023. “Nothing stands still: A spatiotemporal benchmark on 3d point cloud registration under large geometric and temporal change.” *arXiv preprint arXiv:2311.09346*.

Varney, N., V. K. Asari, and Q. Graehling. 2020. “DALES: A large-scale aerial LiDAR data set for semantic segmentation.” In: *Proceedings of the IEEE/CVF conference on computer vision and pattern recognition workshops*, 186–187.

- Wang, C., and Y. K. Cho. 2015. "Smart scanning and near real-time 3D surface modeling of dynamic construction equipment from a point cloud." *Automation in Construction*, 49: 239–249. Elsevier.
- Wang, J., W. Sun, W. Shou, X. Wang, C. Wu, H.-Y. Chong, Y. Liu, and C. Sun. 2015. "Integrating BIM and LiDAR for real-time construction quality control." *Journal of Intelligent & Robotic Systems*, 79 (3): 417–432. Springer.
- Wu, C., Y. Yuan, Y. Tang, and B. Tian. 2021. "Application of terrestrial laser scanning (TLS) in the architecture, engineering and construction (AEC) industry." *Sensors*, 22 (1): 265. MDPI.
- Wu, X., L. Jiang, P.-S. Wang, Z. Liu, X. Liu, Y. Qiao, W. Ouyang, T. He, and H. Zhao. 2024. "Point transformer v3: Simpler faster stronger." In: *Proceedings of the IEEE/CVF conference on computer vision and pattern recognition*, 4840–4851.
- Wu, X., Y. Lao, L. Jiang, X. Liu, and H. Zhao. 2022. "Point transformer v2: Grouped vector attention and partition-based pooling." *Advances in Neural Information Processing Systems*, 35: 33330–33342.
- Xu, J., L. Ding, H. Luo, E. J. Chen, and L. Wei. 2019. "Near real-time circular tunnel shield segment assembly quality inspection using point cloud data: A case study." *Tunnelling and Underground Space Technology*, 91: 102998. Elsevier.
- Zhang, J., X. Zhao, Z. Chen, and Z. Lu. 2019. "A Review of Deep Learning-Based Semantic Segmentation for Point Cloud." *IEEE Access*, 7: 179118–179133. <https://doi.org/10.1109/ACCESS.2019.2958671>.
- Zhao, H., L. Jiang, J. Jia, P. H. S. Torr, and V. Koltun. 2021. "Point transformer." In: *Proceedings of the IEEE/CVF international conference on computer vision*, 16259–16268.
- Zhao, Z.-Q., P. Zheng, S. Xu, and X. Wu. 2019. "Object detection with deep learning: A review." *IEEE transactions on neural networks and learning systems*, 30 (11): 3212–3232. IEEE.
- Zhong, H., H. Wang, Z. Wu, C. Zhang, Y. Zheng, and T. Tang. 2021. "A survey of LiDAR and camera

fusion enhancement.” *Procedia Computer Science*, 183: 579–588. Elsevier.